AD_____

Award Number: W81XWH-04-1-0844

TITLE: Prostate Cancer Progression and Serum SIBLING (Small Integrin Binding N-linked Glycoprotein) Levels

PRINCIPAL INVESTIGATOR: Neal Fedarko, Ph.D.

CONTRACTING ORGANIZATION: Johns Hopkins University School of Medicine
Baltimore, MD 21205

REPORT DATE: October 2005

TYPE OF REPORT: Annual

PREPARED FOR: U.S. Army Medical Research and Materiel Command
Fort Detrick, Maryland 21702-5012

REPORT DOCUMENTATION PAGE

Form Approved
OMB No. 0704-0188

1. REPORT DATE *(DD-MM-YYYY)*	2. REPORT TYPE	3. DATES COVERED *(From - To)*
01-10-2005	Annual	15 Sep 04 – 14 Sep 05

4. TITLE AND SUBTITLE
Prostate Cancer Progression and Serum SIBLING (Small Integrin Binding N-linked Glycoprotein) Levels

5a. CONTRACT NUMBER

5b. GRANT NUMBER
W81XWH-04-1-0844

5c. PROGRAM ELEMENT NUMBER

6. AUTHOR(S)
Neal Fedarko, Ph.D.

E-Mail: ndarko@jhmi.edu

5d. PROJECT NUMBER

5e. TASK NUMBER

5f. WORK UNIT NUMBER

7. PERFORMING ORGANIZATION NAME(S) AND ADDRESS(ES)
Johns Hopkins University School of Medicine
Baltimore, MD 21205

8. PERFORMING ORGANIZATION REPORT NUMBER

9. SPONSORING / MONITORING AGENCY NAME(S) AND ADDRESS(ES)
U.S. Army Medical Research and Materiel Command
Fort Detrick, Maryland 21702-5012

10. SPONSOR/MONITOR'S ACRONYM(S)

11. SPONSOR/MONITOR'S REPORT NUMBER(S)

12. DISTRIBUTION / AVAILABILITY STATEMENT
Approved for Public Release; Distribution Unlimited

13. SUPPLEMENTARY NOTES

14. ABSTRACT

It is the goal of the current research to develop serum measures of a family of proteins that we have termed SIBLINGs (for small integrin binding ligand N-linked glycoproteins) as markers for use in prostate cancer detection and progression by studying a large population of prostate cancer patients, a large normal (cancer-free) population, a population of men with noncancerous prostate disease, and individuals with prostate cancer before, during and after treatment. Blood levels of SIBLING gene family members in normal (n=200) and subjects with diagnosed prostate cancer (n=200) have been measured for most of the five SIBLING proteins. The sensitivity, specificity and predictive value of these markers will be completed once all assays have been finished and the data "secured." Similarly, determining how the levels of SIBLINGs in blood correlate with clinical stage and progression, although underway, requires the completion of each SIBLING assay for all samples. This research will determine whether SIBLING levels in blood (a) have high sensitivity and high specificity for prostate cancer detection, (b) can be measured in a general laboratory setting, and (c) provide useful prognostic information on response to treatment and the likelihood of disease progression.

15. SUBJECT TERMS
Biomarkers, immunoassay, detection, receiver operating, characteristics (ROC), sensitivity, specificity, detection

16. SECURITY CLASSIFICATION OF:			17. LIMITATION OF ABSTRACT	18. NUMBER OF PAGES	19a. NAME OF RESPONSIBLE PERSON
a. REPORT	b. ABSTRACT	c. THIS PAGE			USAMRMC
U	U	U	UU	27	19b. TELEPHONE NUMBER *(include area code)*

Table of Contents

Cover.....1

SF 298.....2

Table of Contents.....3

Introduction.....4

Body.....4

Key Research Accomplishments.....7

Reportable Outcomes.....8

Conclusions.....8

References.....8

Appendices.....9

Introduction

Prostate cancer is the leading cancer diagnosed among men in the United States. Detection is currently based on symptom presentation, physical examination including a digital rectal exam (DRE), measuring serum levels of prostate-specific antigen (PSA) and biopsy. The DRE can not detect certain tumors (that are nonpalpable or physically inaccessible) and PSA levels are elevated in certain non-cancerous conditions (acute prostatitis and benign prostatic hyperplasia). PSA measures have a high rate of false positive test results (the PSA is elevated but no cancer is present). False positives are associated with additional medical procedures, significant financial costs and mental stress. In addition both DRE and PSA can't detect early tumors and are sometimes uninformative in terms of predicting disease progression. Biopsies performed for confirmation of abnormal test results or to follow disease progression or response to treatment can have side-effects that impact profoundly upon the quality of life.

Our hypothesis is that serum levels of a gene family we have been studying are an informative marker for prostate cancer detection and progression. Members of this gene family, termed SIBLINGs for Small Integrin Binding LIgand N-linked Glycoproteins) are induced in different cancers (1) have been shown to bind and modulate matrix metalloproteinase (MMP) activity through both the activation of the latent proenzyme and reactivation of tissue inhibitor of matrix metalloproteinase (TIMP)-inhibited MMP(2). MMPs have a well defined role in tumor angiogenesis, progression and metastasis(3). The biological activity of SIBLINGs and MMPs is consistent with a role for SIBLINGs in early tumor progression. This biological plausibility suggests that the levels of these proteins in blood may be used as not only as adjuncts to conventional detection of prostate cancer, but also as serological markers for prostate cancer progression. A confounding facet of prostate cancer is the variable nature of progression (growth rate, metastasis, etc.) and the absence of non-invasive markers that consistently track with progression. The characterization of novel serum markers whose levels may correlate with disease progression will have a profound effect on current prostate cancer management. The work has the potential to benefit individuals with prostate cancer across the spectrum from early detection to disease progression monitoring and modulating therapy. This is a pre-clinical, translational study that will lay the groundwork for future large scale clinical trials.

Body

Overview:

As of the end of the first year of this grant, Task 1 is almost complete. We have yet to obtain the full complement (200) of serum samples from subjects with diagnosed benign prostatic disease. The analysis of baseline and longitudinal samples in Task 2 are also underway (see sample recruitment, below). We have also spent a considerable effort refining the immunoassay methodology by streamlining sample preparation/extraction (see below).

Statement of Work:

The tasks outlined in the original Statement of Work for the first year were to:

Task 1. To determine the utility of serum SIBLING (BSP, OPN, DMP1 and DSPP) levels in detecting cancer of the prostate (Months 1 - 8):

a. Using competitive ELISAs, measure the distribution of BSP, OPN, DMP1 and DSPP in 200 normal individuals free of prostate cancer.
b. Using competitive ELISAs, measure the distribution of BSP, OPN, DMP1 and DSPP in individuals with prostate cancer.
c. Using competitive ELISAs, measure the distribution of BSP, OPN, DMP1 and DSPP in 200 individuals with benign prostatic disease.
d. Determine sensitivity, specificity, positive and negative predictive values as well as receiver operating characteristic (ROC) curve analyses.

Task 2. To determine the utility of serum SIBLING (BSP, OPN, DMP1 and DSPP) levels in predicting prostate cancer progression (Months 9 – 22):

a. Using competitive ELISAs, measure BSP, OPN, DMP1 and DSPP in baseline samples from 200 prostate cancer patients with clinically characterized stage and progression state.
b. Using competitive ELISAs, measure BSP, OPN, DMP1 and DSPP in longitudinal samples collected yearly after initial diagnosis of prostate cancer in 200 patients.
c. Test for clinical association between serum SIBLING levels and tumor grade, stage and progression.

Task 3. To determine the utility of serum SIBLING (BSP, OPN, DMP1 and DSPP) levels in assessing response to treatment. (Months 23 - 36).

a. Using competitive ELISAs, measure BSP, OPN, DMP1 and DSPP in longitudinal samples from 200 prostate cancer patients undergoing treatment. Treatment: androgen-deprivation therapy (gonadotropin-releasing hormone peptide analogues) with a three year follow-up and serum samples drawn at baseline and every six months (1,400 samples total).
b. Test for statistical association between serum SIBLING levels and prostate cancer progression after treatment.

Progress:

Study Design. Intrinsic to our study design is that the laboratory is blinded to diagnosis and staging data on samples until all samples have been analyzed. The plan is to complete competitive ELSA analyses, "lock down" the raw data and results and only then will the study be unblinded.

Sample recruitment. During the first year of the project, we have obtained a total of 200 normal serum samples and 800 serum samples from subjects diagnosed with prostate cancer. One half of the prostate cancer sera are baseline samples, while the other half are

longitudinal samples. Additional serum samples from individuals with benign prostatic disease are to be available in January 2006.

Immunoassays. The laboratory has operational competitive enzyme-linked immunosorbent assays (ELISAs) for quantitatively determining the levels of bone sialoprotein (BSP), osteopontin (OPN), and dentin sialophosphoprotein (DSPP), dentin matrix protein-1 (DMP1), and matrix extracellular phosphoglycoprotein (MEPE). We have applied the assays to the analysis of prostate cancer serum samples and compared the distribution to that from normal subjects. The assays for OPN have all been completed (Figure 1). While mean OPN levels were significantly different between the two groups, (normal mean = 352 ± 15 ng/ml while prostate cancer group mean = 537 ± 18 ng/ml, $p < 0.001$), there was overlap between the high end of one group and low end of the other group.

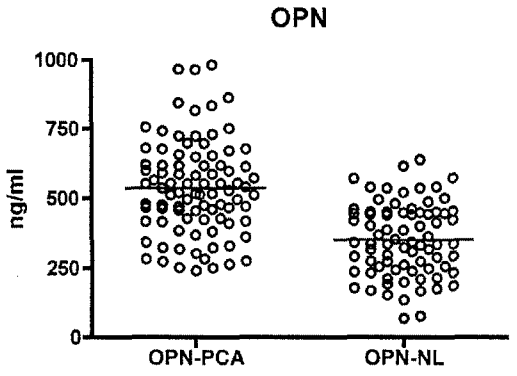

Figure 1. Serum levels of osteopontin in samples from subjects with diagnosed prostate cancer (OPN-PCA) and normal subjects (OPN-NL). A competitive ELISA was used to quantify the amount of osteopontin in serum following sample extraction and clean-up (4).

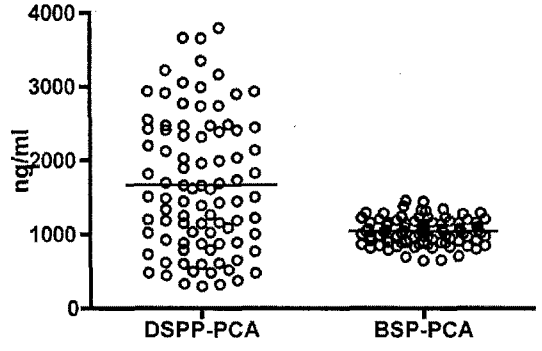

Figure 2. Serum levels of dentin sialophosphoprotein (DSPP) and bone sialoprotein (BSP) in samples from subjects with diagnosed prostate cancer (DSPP-PCA, BSP-PCA). A competitive ELISA was used to quantify the amount of DSPP and BSP in serum.

We have also determined the distribution of BSP and DSPP in the same serum samples from subjects with diagnosed prostate cancer but have not been completed the corresponding normal group serum samples (Figure 2). Past work (published in 2001) with normal sera yielded a mean value of 114 ± 8 ng/ml for BSP (4). For DSPP, comparisons with historical normal sera mean values can not be directly done as the standard employed in the assays has changed. Our initial studies with DSPP used a bacterial recombinant protein fragment of DSPP, while more recent assays have

employed adenoviral-produced recombinant human DSPP. We are currently using the new standard for DSPP analysis of our normal serum bank.

A number of issues have arisen concerning the current competitive immunoassays. One issue is that stability tests over the past year revealed a change occurred in microtiter plate chemistries. We have had to switch microtiter plate manufacturer's (from Greiner Bio-One high binding plates to Costar ELISA/RIA high binding plates. This was necessitated by a change in Greiner's manufacturing process that altered the surface charge/properties of their plates that adversely effected SIBLING protein binding. We rescreened a number of manufacturer's 96 well plates to obtain binding profiles and standard curves closes to those obtained with the "old" plates.

A second issue arises from the nature of the serum sample preparation prior to the immunoassay. Because SIBLINGs are bound in blood/serum/plasma to complement Factor H (very abundant at ~ 0.5 mg/ml), to detect the SIBLINGs we need to disrupt the complex. The complex is disrupted through a combination of chaotropic agents, heating and reduction so that sample clean-up prior to the immunoassay is required. We have been investigating alternative methods of sample preparation and clean-up for their yield and speed (the current standard method uses standard column chromatography for removing reducing and chaotropic agents). The new modified assay entails spiking serum with mucin prior to analysis. Mucin contains sialic acid moieties that confer a tight interaction with complement Factor H and this is being exploited to disrupt the SIBLING-Factor H interaction.

Key Research Accomplishments

Assay Application:
- Competitive ELISAs
  - 200 baseline samples from subjects diagnosed with prostate cancer
    - BSP, OPN, DMP1, DSPP and MEPE
  - 200 samples from subjects with clinically characterized stage and progression state.
    - BSP, OPN, and DMP1
  - 200 samples from normal subjects
    - OPN, DMP1 and MEPE

Assay Modification:
- Alternative serum processing
  - Replacing sample reduction & column chromatography with "mucin displacement buffer" treatment of serum.

Submitted Manuscripts:

Jain, A., Fisher, L.W. and N.S. Fedarko. (2005) Bone Sialoprotein Binding To Matrix Metalloproteinase-2 Alters Enzyme Inhibition Kinetics. J. Biol. Chem.

Reportable Outcomes

Invited Presentations:

"The SIBLING gene family promotes tumor progression." 2004-2005 Johns Hopkins University Oncology Translational Research Conference, November 3rd, 2004, Baltimore, MD

"SIBLING modulation of matrix metalloproteinases and tumor progression." 2nd National Meeting of the American Society for Matrix Biology. November 12, 2004, San Diego, CA.

"What do bone proteins have to do with tumor progression?" The Sidney Kimmel Comprehensive Cancer Center At Johns Hopkins Longrifles Seminar Series, March 2nd, 2005, Baltimore MD.

"MMP activation by SIBLINGs" Gordon Research Conference on Small Integrin-Binding Proteins, September 12th, 2005 Big Sky, MT

- Funding Applied For
  - NCI Small integrin-binding proteins and tumor progression.

Conclusions

Before the data and results are "locked down," we need to complete the analysis of the large normal group for BSP and DSPP. In addition, the samples from subjects with diagnosed prostate cancer and defined staging need to have the MEPE measurements completed and the longitudinal samples collected yearly post diagnosis need to be completed for the SIBLINGs analysis. The completion of the final parts of Tasks 1 and 2 (determining sensitivity, specificity and association between serum SIBLINGs levels and tumor grade and progression must wait until once the data set is complete and locked down. The laboratory is on track to complete these Tasks by the end of year 2 of the award.

References

1. Fisher LW, Jain A, Tayback M, Fedarko NS. Small Integrin Binding LIgand N-linked Glycoprotein (SIBLING) gene family expression in different cancers. Clin Can Res 2004;10(24):8501-11.
2. Fedarko NS, Jain A, Karadag A, Fisher LW. Three small integrin binding ligand N-linked glycoproteins (SIBLINGs) bind and activate specific matrix metalloproteinases. Faseb J 2004;18(6):734-6.
3. Freije JM, Balbin M, Pendas AM, Sanchez LM, Puente XS, Lopez-Otin C. Matrix metalloproteinases and tumor progression. Adv Exp Med Biol 2003;532:91-107.
4. Fedarko NS, Jain A, Karadag A, Van Eman M, Fisher LW. (2001) Elevated serum bone sialoprotein and osteopontin in colon, breast, prostate and lung cancer. Clin. Cancer Res. 7:4060-4066.

Appendix

Jain, A., Fisher, L.W. and N.S. Fedarko. (2005) Bone Sialoprotein Binding To Matrix Metalloproteinase-2 Alters Enzyme Inhibition Kinetics. J. Biol. Chem.

BONE SIALOPROTEIN BINDING TO MATRIX METALLOPROTEINASE-2 ALTERS ENZYME INHIBITION KINETICS.

Alka Jain*, Larry W. Fisher#, and Neal S. Fedarko*

From the *Department of Medicine, Johns Hopkins University, Baltimore, MD 21224 and #Craniofacial and Skeletal Diseases Branch, NIDCR, NIH, DHHS, Bethesda, MD. 20892.

Bone sialoprotein (BSP) is induced by multiple neoplasms *in vivo,* its expression levels correlate with tumor stage and it can modulate the activity of matrix metalloproteinase-2 (MMP-2). In this study, the hypothesis that BSP acts biologically to lessen the effectiveness of MMP inhibitors was investigated. Solution and solid phase binding assays were carried out demonstrating that binding between recombinant BSP and latent as well as active MMP-2 does not require the hemopexin domain. BSP binding restored activity to hemopexin-deleted MMP-2 inhibited by tissue inhibitor of matrix metalloproteinase-2 (TIMP2) when activity was measured using both natural, large macromolecular substrates and synthetic, small molecular weight, freely diffusable substrates. BSP effects on TIMP2 inhibition of wild type active MMP-2 were quantified by varying small molecular weight substrate concentrations at different fixed inhibitor concentrations, and solving a general linear mixed inhibition rate equation with a global curve fitting program. The results indicate a 15 to 30-fold increase in the competitive inhibition constant and an ~ 6-fold increase in uncompetitive inhibition constant for the MMP-2+BSP complex. To address whether the failure of clinical trials of MMP inhibitors may be explained at least in part by the activity of BSP, the effect of BSP binding to MMP-2 on inhibition by a small molecular weight drug (illomastat) was similarly determined. An over 30-fold increase in K_I was observed. The ability of BSP to modulate MMP inhibitor action in an *in vitro* angiogenesis model system was tested. When human umbilical vein endothelial cells co-cultured with dermal fibroblasts in defined medium were treated with either nM TIMP2 or illomastat, the degree of tubule formation was reduced while the addition of equimolar BSP restored vessel formation.

The Small Integrin Binding LIgand N-linked Glycoprotein (SIBLING) gene family is clustered on human chromosome 4 and its members include bone sialoprotein (BSP), osteopontin, dentin matrix protein 1, matrix extracellular phosphoglycoprotein, and dentin sialophosphoprotein (1). BSP was once thought to be restricted in expression to mineralizing tissue such as bones and teeth (2) but has recently been shown to be expressed in ductal elements of salivary gland (3) and kidney (4). SIBLINGs, including BSP, are also induced in certain neoplasms (5-15). SIBLINGs can be co-localized to the cell surface through binding of $\alpha_V\beta_3$ and/or CD44 (16-18); exhibit correlation between expression levels and tumor stage (19); and bind and modulate the activity of different but specific matrix metalloproteinases (MMP)s (20). Indeed, BSP has been shown to enhance the invasion potential of many human cancer cell lines in vitro by bridging MMP-2 to the cell surface of the cells through the $\alpha_V\beta_3$ integrin (18).

MMPs are a family of structurally and functionally related endoproteinases that are involved in development and tissue repair as well as cancer angiogenesis and metastasis. We have recently shown that active MMPs inhibited by either tissue inhibitors of MMPs (TIMPs) or low molecular weight synthetic inhibitors can be reactivated by equimolar amounts of the appropriate SIBLING partner (20). The current study was undertaken to determine whether BSP action on MMP-2 inhibition involves the hemopexin domain, and to see if the SIBLING alters MMP affinity for substrates, TIMP2 or small molecular weight inhibitors. The biological consequences of these interactions were tested in an *in vitro* model system of angiogenesis.

Materials and Methods

Reagents. Pro- and active human MMP-2 was obtained from Oncogene Research Products (Boston, MA) and Research Diagnostic Systems, Inc. (Minneapolis, MN). Recombinant human

MMP-2 lacking the hemopexin domain was purchased from Biomol Research Laboratories, Inc. (Plymouth Meeting, PA). The inhibitor illomastat (GM6001, or N-[(2R)-2-(hydroxamido-carbonylmethyl)-4-methylpentanoyl]-L-tryptophan methylamide), substrate Ac-PLG-[2-mercapto-4-methyl-pentanoyl]-LG-OC_2H_5 , and 5,5'-dithio-bis-2-nitrobenzoic acid (DTNB) were obtained from Calbiochem (La Jolla, CA). TIMP2 was a generous gift of Dr. H. Birkedal-Hansen, NIDCR, NIH. Human serum adsorbed goat anti-rabbit IgG conjugated to horseradish peroxidase (HRP) was obtained from Kirkegaard & Perry (Gaithersburg, MD). Recombinant human BSP that included post translational modifications was made using an adenovirus construct and eukaryotic cells and purified (> 95% purity as defined by acrylamide gel electrophoresis) as previously described (16).

Fluorescent binding studies. Intrinsic tryptophan fluorescence binding studies of BSP and mutant hemopexin-deleted MMP-2 were carried out as previously described (20). BSP contains no tryptophan groups while the hemopexin-deleted MMP-2, contains 8, so the intrinsic fluorescence changes are a result of the change in conformation of the MMP alone. Briefly, the relative change in fluorescence in the area under the emission curve (300 to 500 nm at 295 nm excitation) was used to determine binding curves. Fractional acceptor saturation (f_a) as a function of nM BSP added was determined by calculating $f_a = (y - y_f)/(y_b - y_f)$, where y_f and y_b are the area under the curve of the fluorescent emission profile of free and fully bound MMP-2. Scatchard plots were made by fitting the transformed data to the function $r/[BSP] = n/K_d - r/K_d$., where r represents the binding function, $[BSP]$, BSP concentration, n the number of binding sites and K_d the dissociation constant.

Solid phase binding assays. The binding of BSP to purified and immobilized MMP-2 was measured by an indirect sandwich assay. Plates were coated with the different forms of MMP-2 by adding 0.1 ml of 3.5 nM recombinant purified MMP-2 in 50 mM $NaHCO_3$, pH 9.0 to each well of a Greiner high-binding 96-well microtiter plates (stock # 655061, Greiner Bio-One, Longwood, FL) incubated overnight at 4°C. The plates were blocked with 5 % (w/v) nonfat dry milk in TBS for 60 min and then rinsed three times with TBS containing 0.05 % Tween 20. BSP was added in nM equivalents in TBS-Tween and incubated for 120 min at room temperature. After a second round of three washes, bound ligand was quantified by the addition of a 1:50,000 dilution of specific rabbit anti-BSP antibody, LF100 (21), followed by a 60 min incubation. After three washes, secondary antibody (1:2000 goat anti-rabbit horseradish peroxidase conjugated antibody) was added and incubated for a further 60 min. Color was developed using diaminobenzamidine substrate and the absorbance at 405 nm was measured. Non-specific binding was measured by determining the ligand binding to wells coated with BSA alone, and these values were subtracted from the corresponding values for MMP-coated wells.

High molecular weight substrate studies. Fluorescein-conjugated gelatin (Molecular Probes, Inc., Eugene, OR) substrate was used to follow proteolytic activity as previously described (20). This substrate is highly substituted with fluorescein moieties so that the fluorescent signal is self-quenched until proteolytic cleavage liberates fragments and a robust fluorescent emission is measured. The reaction mixture consisted of the fluorescein-substrate conjugate with 1.4 nM mutant hemopexin-free MMP-2 reacted with either 10 nM TIMP2, 10 nM TIMP2 + 10 nM BSP, 10 nM BSP, or buffer alone (50 mM Tris, pH 7.6, 150 mM NaCl, 5 mM $CaCl_2$). Relative velocity plots were determined by varying the substrate concentration between 0.025 and 15 μg/ml and determining the change in fluorescence over the first hour of reaction. Inhibitor titrations were carried out by varying TIMP2 concentration from 1.6 to 1600 nM. Fluorescent data was acquired with excitation at 485 nm and emission at 535 nm. Reactions were run in duplicate.

Low molecular weight substrates. The activities of mutant and wild type MMP-2 in the presence and absence of inhibitors (TIMP2 or illomastat) and BSP were measured using a small molecular weight thiopeptide substrate (Ac-PLG-[2-mercapto-4-methyl-pentanoyl]-LG-OC_2H_5). Substrate was incubated in assay buffer (50 mM HEPES, 10 mM $CaCl_2$, 0.05% Brij-35, 1 mM

DTNB, pH 7.5) with 10 nM MMP-2 + different concentrations of inhibtor, a 10 nM [MMP-2+BSP] preformed complex or MMP2 + inhibitor + BSP added simultaneously. Data from the first six minutes were used to calculate velocity (pmols/sec) values. Substrate cleavage was monitored using a Perkin Elmer Victor 2 multilabel plate reader and absorbance was measured at 412 nM. Preformed complexes of [MMP-2+BSP] were formed by incubation at 37 C for 30 minutes prior to addition to the reaction mixture. Global curve-fitting of the family of substrate-velocity curves was performed using Prism 4 software (GraphPad Software, Inc.,) with V_{max}, K_m, K_{ic} and K_{iu} set as shared parameters.

SDS PAGE, zymography. 10% zymogram gelatin gels were obtained from Invitrogen, Inc., (Carlsbad, CA). Samples in zymogram gel sample buffer were electrophoresed at a constant 125 V for 90 min. Gels were processed for zymography according to the manufacture's instructions, stained with 0.5% Coomassie Brilliant Blue R250, and bands were visualized by dynamic integrated exposure using an AlphaInotech imaging system (Alpha Inotech Corp., San Leandro, CA).

In vitro angiogenesis. Human umbilical vein endothelial cell (HUVEC) and human dermal fibroblast co-cultures and EGM-2 defined medium were obtained from TCS Cell Works (Botolph Claydon, UK). The functional readout from this *in vitro* assay was tubule formation. Tubule formation was defined by the total number of tubules, total tubule length, mean tubule length, and number of branches. Test conditions were run in triplicate wells with 8 conditions per 24 well plate. The cells were treated starting on day six of culture with 5 nM BSP, 5 nM TIMP2, 5 nM BSP + TIMP2, 5 nM GM6001, 5 nM GM6001 + BSP, or buffer alone. Medium was changed every other day with fresh medium containing experimental conditions. Cells were fixed in 70 % ethanol on day 12 and tubule formation was quantified following immunostaining with a mouse anti-human PECAM-1 monoclonal antibody (TCS Cell Works), and the secondary antibody being goat anti-mouse IgG alkaline phosphatase coupled antibody, with 5-bromo-4-chloro-3-indolyl phosphate/ nitro blue tetrazolium (BCIP/NBT; Sigma) as substrate. Images were visualized on a Nikon Diaphot inverted microscope and digitized with a Polaroid CCD digital camera and software. Two images per well were captured, digitized and the number of tubules, the number of branch points (junctions) between tubules, as well as the total tubule length (in pixels) determined using AngioSys Version 1.0 software. (TCS Cell Works, Botolph Claydon, UK).

For zymographic analyses of MMP-2, a membrane-associated fraction was prepared from the HUVEC cocultures essentially as described by Ward et al. (22). Briefly, HUVEC cells were scraped from culture wells in cold 5 mM Tris HCl (pH 7.8), homogenized, and crude membranes were prepared by centrifugation of the cell lysate at 10,000 x g for 15 minutes at 4°C. The supernatant was centrifuged at 105,000 x g for 1 hour at 4°C; then, the supernatant was removed and saved, and the membrane fraction was resuspended in 20 mM Tris HCl (pH 7.8), 10 mM $CaCl_2$, and 0.05% Brij 35.

RESULTS

Bone sialoprotein binding does not require the hemopexin domain. MMPs consist of a catalytic domain and a hemopexin-like domain thought to be essential for the binding of many natural substrates. TIMPs have binding sites in both the hemopexin and catalytic domains (23). We have shown previously that BSP can bind to both pro- and active MMP-2 (20). Whether BSP interacts with the hemopexin domain or, at least in part, with the catalytic region was investigated by studying the binding characteristic of BSP to recombinant human MMP-2 that lacks the hemopexin domain. When the intrinsic tryptophan fluorescence of the mutant MMP-2 was followed during titration with BSP, quenching of the signal similar to that previously seen for the intact MMP-2 was observed (Fig. 1). The area under the emission peaks was quantified and used to determine the change in fluorescence and calculate both the fractional acceptor saturation as a function of nM BSP added and a corresponding Scatchard plot. BSP binding was saturable and its affinity for the mutant protein was actually higher than that for intact MMP-2 (K_d = 0.07 ± 0.03 nM for mutant MMP-2 versus 0.32 ± 0.02 nM for active MMP-2, and 2.9 ± 0.9 nM for pro-MMP-2).

An alternative method to confirm BSP and MMP-2 binding was employed. Solid phase binding assays were developed to measure BSP binding to immobilized forms of MMP-2. Microtiter plates coated with either proMMP-2, active MMP-2 or hemopexin-deleted MMP-2 were reacted with increasing concentrations of BSP and the amount bound quantified by specific antibodies (Fig. 1D). The binding of BSP to MMP variants was saturable. Scatchard plot analysis revealed BSP binding with a K_d = 0.39 ± 0.04 nM for mutant MMP-2 versus 0.36 ± 0.04 nM for active MMP-2 and 2.1 ± 0.1 nM for pro- MMP-2 (Fig. 1E). While the pro- and active forms of MMP-2 exhibited essentially similar binding constants by the two different binding methods, the mutant form of MMP-2 exhibited a distinct K_d value which may be reflecting differences in solid phase binding orientation in the absence of the hemopexin domain. Attempts to measure BSP binding to TIMP2 by either intrinsic tryptophan fluorescence spectroscopy (TIMP2 contains 4 internal tryptophans, BSP none) or by solid phase binding assay were negative (data not shown).

Bone sialoprotein modulation of MMP-2 activity does not require the hemopexin domain. We recently reported that BSP can restore enzymatic activity to MMP-2 incubated with TIMP2 when activity was followed using a natural, large molecular weight substrate (gelatin) (20). The effect of BSP on the activity of the mutant MMP-2 was therefore investigated using the gelatin-fluorescein large molecular weight substrate assay (Fig. 2 A-D). The change in substrate fluorescence caused by mutant MMP-2 alone compared to a complex of equimolar mutant MMP-2 + BSP was not significantly different. As expected, the addition of equimolar TIMP2 to mutant MMP-2 caused a significant decrease in the rate of fluorescence change. However, inclusion of equimolar BSP to mutant MMP-2 + TIMP2 complexes restored the rate of fluorescence change to that of mutant MMP-2 alone showing that the TIMP2 became ineffective in the presence of bound BSP. Substrate velocity plots as a function of substrate concentration yielded no significant difference for mutant MMP-2 in the presence or absence of BSP. Titration with TIMP2 of mutant MMP-2 and the large molecular weight substrate revealed that over a 100-fold excess of TIMP2 was required to inhibit activity to 20 % (Fig. 2 C). For complexes of equimolar mutant MMP-2 + TIMP2, the rate of the reaction was decreased to 67 %, while the presence of equimolar BSP restored activity to 97 %. Increasing the concentration of BSP in mixes of equimolar TIMP2 and mutant MMP-2 further increased the reaction rate (Fig. 2 D).

A low molecular weight freely diffusible peptide substrate assay was next used and enabled kinetic parameters to be evaluated (Fig. 2 E-H). Similar to results with the large molecular weight substrate, the addition of BSP alone did not significantly alter mutant MMP-2 enzyme product evolution. Furthermore, the TIMP2 inhibited product evolution as expected and the addition of BSP to the preformed mutant MMP-2/TIMP2 complex returned the digestion to uninhibited levels. Substrate velocity plots of mutant MMP-2 ± BSP yielded no statistically significant difference in fitted K_m or v_{max} values (Table I) verifying the observations with the larger substrate that the conformational changes induced by BSP did not significantly affect the actions of the active site itself. Titration of the small molecular weight substrate and mutant MMP-2 with varying concentrations of TIMP2 indicated that at 10-fold excess, TIMP2 inhibited mutant MMP-2 activity to 20 %, while equimolar TIMP2 inhibited mutant MMP-2 and to 34 % (Fig. 2 G). The addition of equimolar BSP was able to restore the activity of mutant MMP-2 treated with TIMP2 to 85 %. Increasing the concentration of BSP in reaction mixtures of small molecular weight substrate + equimolar TIMP2 and mutant MMP-2 restored activity further (Fig. 2 H). These data suggest that BSP reactivation of TIMP2-inhibited MMP-2 does not require the hemopexin domain of MMP-2.

TIMP Inhibition kinetics. To determine the effect of BSP on active wild type MMP-2 and TIMP2 reaction kinetics, the small molecular weight substrate was employed to follow product evolution over time. MMP-2 incubated with increasing concentrations of TIMP2 exhibited the expected dose-dependent inhibition (Fig. 3A). The inhibition by TIMP2 was significantly decreased by the presence of either a performed complex of [MMP-2+BSP] or by the simultaneous addition of BSP and TIMP2 to MMP-2 (Fig. 3B, C). To

investigate whether decreased inhibition of MMP-2 by TIMP2 in the presence of BSP was associated with an altered affinity, substrate-velocity plots were obtained by varying substrate concentrations of each at different but fixed inhibitor concentrations. Reaction conditions included either TIMP2 + 10 nM MMP-2, TIMP2 + preformed equimolar complexes of 10 nM [MMP-2+BSP], or simultaneous mixes of TIMP2 + 10 nM MMP-2 + 10 nM BSP (Fig. 3D - E).

Because there are two distinct binding sites for TIMP2 on MMP-2, TIMP2 does not act purely as a competitive inhibitor (24). The common types of inhibition (competitive, uncompetitive, noncompetitive) are all special cases of linear mixed inhibition (25). The generalized linear mixed inhibition equation $v = V_{max}[S]/\{K_m(1+ [I]/K_{ic}) + [S](1+[I]/K_{iu})\}$, was employed to determine the reaction rate. V_{max} is the limiting rate, K_m is the Michaelis constant, K_{ic} is the competitive inhibition constant and K_{iu} is the uncompetitive inhibition constant. For competitive inhibition, $[I]/K_{iu}$ is negligible while for uncompetitive inhibition $[I]/K_{ic}$ is negligible. In pure noncompetitive inhibition the inhibition constants are equal.

Global curve-fitting of the family of substrate-velocity curves (Fig. 3D-F) revealed a significant increase in K_{ic} and K_{iu} values for the [MMP-2+BSP] complex as well as the simultaneously added MMP-2 + BSP (Table I). This indicates a relatively poor affinity of the inhibitor for MMP-2 in the presence of BSP. The order of magnitude change in apparent inhibitor affinity for MMP-2 in the presence of BSP indicates that SIBLING modulation of MMPs is physiologically significant.

Illomastat inhibitor kinetics. The MMP inhibitor illomastat was utilized to test whether small molecular weight drug inhibition of MMP-2 activity could be modulated by BSP. Illomastat at a 1 nM concentration inhibited the initial velocity of MMP-2 activity to 39 % of control activity, while the same concentration of inhibitor reduced the activity of the MMP-2 + BSP to only 70 % of control suggesting that the inhibitor is much less effective against MMP-2 in the conformation resulting from the binding of BSP (Figure 4A). Titration of a mix of 10 nM MMP-2 + 1 nM illomastat with increasing concentrations of BSP revealed a dose-dependent decrease to the inhibitor's action (Fig. 4B).. To quantify the effects of BSP on MMP-2 inhibitor kinetics, substrate-velocity plots were obtained by varying substrate concentrations of each at different but fixed illomastat concentrations. Reaction conditions were either 10 nM MMP-2 alone, or with 10 nM equimolar MMP-2 + BSP (Fig. 4C, D).

Because Illomastat is a competitive inhibitor, kinetic parameters in the presence and absence of BSP can be determined by fitting the substrate-velocity curves to the equation for competitive inhibition: $v = v_{max}[S]/K_m(1+[I]/K_{Ic})+[S]$; where V_{max} is the limiting rate, K_m is the Michaelis constant, K_{Ic} is the competitive inhibition constant, $[S]$ is substrate concentration and $[I]$ is illomastat concentration. The results indicated a significant increase (> 30-fold) in K_{Ic} value for the MMP-2 + BSP (Table I). Thus illomastat exhibited a reduced affinity for MMP-2 in the presence of BSP.

BSP restores activity to inhibited MMPs in vitro. The ability of BSP to restore enzymatic activity to TIMP2- and illomastat-inhibited MMP-2 in a purified component assay led to a screen of the effects of BSP on MMP inhibitors in an *in vitro* angiogenesis system. 5 nM BSP alone stimulated tubule formation by HUVEC cells while separately illomastat (GM6001) and TIMP2 inhibited tubule formation below control levels (Figure 5). The inclusion of BSP with MMP-specific inhibitors restored tubule formation. Quantification of tubule formation using AngioSys Ver. 1.0 software revealed that the addition of BSP to TIMP2 or illomastat-treated cells restored not only the number of tubules but also the number of branch points and total tubule length (in pixels) to values not significantly different from BSP enhancement alone (Figure 6). The effect of BSP on MMP-2 levels and activity in the *in vitro* angiogenesis system was also studied by two other, complementary systems. MMP activity measured by the fluorescein-gelatin substrate assay and a rate of digestion of gelatin by zymography. Both assays exhibited a consistent

pattern of increased enzymatic activity in BSP-treated conditions.

DISCUSSION

BSP is a member of the SIBLING gene family (2). It is extended and flexible in solution and such lack of ordered structure is shared by a number proteins that have multiple binding partners (1). BSP can bind the $\alpha_V\beta_3$ integrin via its RGD sequence (26,27) and to complement Factor H (16). BSP can also bind to and modulate the activity of MMP-2 (20). Binding of BSP to MMP-2 was associated with conformational changes as indicated by fluorescent quenching during BSP binding titration (indicating a change in the microenvironment of the MMP's tryptophans); and by increased susceptibility of a BSP–proMMP-2 complex to plasmin cleavage. BSP binding to latent MMP-2 was associated with increased proteolytic activity and BSP binding to TIMP2-inhibited MMP-2 restored activity (20). Taken together the data suggest that conformational changes in MMP-2 induced by BSP binding may include changes in the shape of the active site and inhibitor binding domains. A trimolecular complex of BSP, $\alpha_V\beta_3$ and MMP-2 can be demonstrated by immunoprecipitation, flow cytometry, and *in situ* hybridization in cancer cells grown *in vitro* (18). BSP message was induced in multiple cancers and its expression correlated with paired MMP-2 expression as well as tumor stage (19).

MMP-2, a gelatinase that can degrade components of the extracellular matrix at physiological pH, is regulated *in vivo* by the naturally occurring TIMPs and RECK (28,29). TIMP2 binding to MMP-2 involves distinct domains on both the inhibitor and the enzyme (30-32). The binding and kinetics of MMP-2 and TIMP2 are more complex than simple competitive inhibition. In our analyses we have used a mixed linear model of mixed inhibition (25) and observed inhibition constants in the $\leq$ nM range. K_I values in sub-nanamolar range for TIMP2 and MMP-2 using the same substrate have been reported in the literature (33-35), though a more recent analysis has yielded 3- to 4-fold higher estimation (23). The different reported values are most likely due to differences in sources and concentrations of substrate, enzyme and inhibitor.

SIBLING binding to active MMPs inhibited by TIMP or small molecular weight MMP-specific inhibitors could restore activity through multiple mechanisms. Possible mechanisms include blocking inhibitor access (steric blocking), binding to the inhibitor (stripping), or by altering inhibitor affinity. The analysis of inhibitor kinetic parameters as well as binding order effects can be used to distinguish between steric blocking or affinity changes. Based on the current studies with BSP, MMP-2 and TIMP2, SIBLING binding to MMP did not significantly alter K_m values but did alter the MMP's affinity for its inhibitor. SIBLING binding to inhibitor (stripping) was not observed.

BSP was found to significantly reduce the affinity of a small molecular weight synthetic inhibitor (illomastat) for MMP-2. Illomastat as a hydroxamate class inhibitor blocks the activity of multiple MMPs and has been used to disrupt angiogenesis and metastasis (36-38). Illomastat blocked TNFα processing (39), experimental autoimmune encephalitis (40), angiogenesis and metastasis (36-38). The magnitude of change in apparent inhibitor affinity for MMP-2 in the presence of BSP indicates that SIBLING modulation of MMP inhibition by small molecular weight drugs can be physiologically significant.

Finally, a cell culture model system was used to test whether BSP modulation of MMP-2 inhibition occurs *in vitro*. The *in vitro* model of angiogenesis utilized human umbilical vein endothelial cells (HUVECs) co-cultured with normal adult human diploid dermal fibroblasts. The endothelial cells form small islands amongst the fibroblasts, proliferate, and migrate through the co-culture matrix to form thread-like tubule structures. These cord-like structures join up to form a network of anastomosing tubules. These linked tubules produce endothelial cell-specific components such as von Willebrand Factor and PECAM-1 (CD31) that can be stained immunohistochemically and quantified. The observed effects of BSP (stimulating basal tubule formation and restoring formation to TIMP2- or illomastat-inhibited cultures) was consistent with BSP modulating MMP-2 activity. Profiling MMP-2 levels and activity in the *in vitro* system (by

zymography and fluorescent substrate assays) demonstrated changes with BSP treatment. BSP has been shown to promote angiogenesis in the chick chorioallantoic membrane system (41). Thus, BSP has biochemical and biological plausibility to be playing active roles in tumor progression *in vivo*. BSP is induced by multiple neoplasms *in vivo* and its modulation of MMP activity might contribute to the relative lack of efficacy seen in the recent clinical trials of MMP inhibitors in numerous cancers (42).

Literature Cited

1. Fisher, L. W., Torchia, D. A., Fohr, B., Young, M. F., and Fedarko, N. S. (2001) *Biochem. Bophys. Res. Comm.* **280**, 460-465
2. Fisher, L. W., and Fedarko, N. S. (2003) *Connect Tissue Res* **44 Suppl 1**, 33-40
3. Ogbureke, K. U., and Fisher, L. W. (2004) *J Dent Res* **83**(9), 664-670
4. Ogbureke, K. U., and Fisher, L. W. (2005) *Kidney Int* **68**(1), 155-166
5. Craig, A. M., Bowden, G. T., Chambers, A. F., Spearman, M. A., Greenberg, A. H., Wright, J. A., McLeod, M., and Denhardt, D. T. (1990) *Int J Cancer* **46**(1), 133-137
6. Gillespie, M. T., Thomas, R. J., Pu, Z. Y., Zhou, H., Martin, T. J., and Findlay, D. M. (1997) *Int J Cancer* **73**(6), 812-815
7. Hirota, S., Nakajima, Y., Yoshimine, T., Kohri, K., Nomura, S., Taneda, M., Hayakawa, T., and Kitamura, Y. (1995) *J Neuropathol Exp Neurol* **54**(5), 698-703
8. Senger, D. R., Perruzzi, C. A., and Papadopoulos, A. (1989) *Anticancer Res* **9**(5), 1291-1299
9. Sung, V., Stubbs, J. T., 3rd, Fisher, L., Aaron, A. D., and Thompson, E. W. (1998) *J Cell Physiol* **176**(3), 482-494
10. Bellahcene, A., Kroll, M., Liebens, F., and Castronovo, V. (1996) *J Bone Miner Res* **11**(5), 665-670
11. Bellahcene, A., Albert, V., Pollina, L., Basolo, F., Fisher, L. W., and Castronovo, V. (1998) *Thyroid* **8**(8), 637-641
12. Bellahcene, A., Merville, M. P., and Castronovo, V. (1994) *Cancer Res* **54**(11), 2823-2826
13. Bellahcene, A., Maloujahmoum, N., Fisher, L. W., Pastorino, H., Tagliabue, E., Menard, S., and Castronovo, V. (1997) *Calcif Tissue Int* **61**(3), 183-188
14. Chaplet, M., De Leval, L., Waltregny, D., Detry, C., Fornaciari, G., Bevilacqua, G., Fisher, L. W., Castronovo, V., and Bellahcene, A. (2003) *J Bone Miner Res* **18**(8), 1506-1512
15. Rowe, P. S., de Zoysa, P. A., Dong, R., Wang, H. R., White, K. E., Econs, M. J., and Oudet, C. L. (2000) *Genomics* **67**(1), 54-68
16. Fedarko, N. S., Fohr, B., Gehron Robey, P., Young, M. F., and Fisher, L. W. (2000) *J. Biol. Chem.* **275**, 16666-16672
17. Jain, A., Karadag, A., Fohr, B., Fisher, L. W., and Fedarko, N. S. (2002) *J Biol Chem* **277**(16), 13700-13708
18. Karadag, A., Ogburke, K. U. E., Fedarko, N. S., and Fisher, L. W. (2004) *J. Natl. Cancer Inst.* **96**(12), In press.
19. Fisher, L. W., Jain, A., Tayback, M., and Fedarko, N. S. (2004) *Clin. Can. Res* **10**(24), 8501-8511
20. Fedarko, N. S., Jain, A., Karadag, A., and Fisher, L. W. (2004) *Faseb J* **18**(6), 734-736
21. Mintz, K. P., Grzesik, W. J., Midura, R. J., Robey, P. G., Termine, J. D., and Fisher, L. W. (1993) *J Bone Miner Res* **8**(8), 985-995
22. Ward, R. V., Atkinson, S. J., Slocombe, P. M., Docherty, A. J. P., Reynolds, J. J., and Murphy, G. (1991) *Biochim Biophys Acta.* **1079**, 242 –246.
23. Olson, M. W., Gervasi, D. C., Mobashery, S., and Fridman, R. (1997) *Journal of Biological Chemistry* **272**, 29975-29983.

24. Kleiner, D. E., Jr., Unsworth, E. J., Krutzsch, H. C., and Stetler-Stevenson, W. G. (1992) *Biochemistry* **31**(6), 1665-1672
25. Cortes, A., Cascante, M., Cardenas, M. L., and Cornish-Bowden, A. (2001) *Biochem J* **357**(Pt 1), 263-268
26. Oldberg, A., Franzen, A., and Heinegard, D. (1986) *Proc Natl Acad Sci U S A* **83**(23), 8819-8823
27. Fisher, L. W., McBride, O. W., Termine, J. D., and Young, M. F. (1990) *J Biol Chem* **265**(4), 2347-2351
28. Giannelli, G., and Antonaci, S. (2002) *Histol Histopathol* **17**(1), 339-345
29. Oh, J., Takahashi, R., Kondo, S., Mizoguchi, A., Adachi, E., Sasahara, R. M., Nishimura, S., Imamura, Y., Kitayama, H., Alexander, D. B., Ide, C., Horan, T. P., Arakawa, T., Yoshida, H., Nishikawa, S., Itoh, Y., Seiki, M., Itohara, S., Takahashi, C., and Noda, M. (2001) *Cell* **107**(6), 789-800
30. Willenbrock, F., Crabbe, T., Slocombe, P. M., Sutton, C. W., Docherty, A. J., Cockett, M. I., O'Shea, M., Brocklehurst, K., Phillips, I. R., and Murphy, G. (1993) *Biochemistry* **32**(16), 4330-4337
31. Nguyen, Q., Willenbrock, F., Cockett, M. I., O'Shea, M., Docherty, A. J., and Murphy, G. (1994) *Biochemistry* **33**(8), 2089-2095
32. Hutton, M., Willenbrock, F., Brocklehurst, K., and Murphy, G. (1998) *Biochemistry* **37**(28), 10094-10098
33. O'Shea, M., Willenbrock, F., Williamson, R. A., Cockett, M. I., Freedman, R. B., Reynolds, J. J., Docherty, A. J., and Murphy, G. (1992) *Biochemistry* **31**(42), 10146-10152
34. Murphy, G., and Docherty, A. J. (1992) *Am J Respir Cell Mol Biol* **7**(2), 120-125
35. O'Connell, J. P., Willenbrock, F., Docherty, A. J., Eaton, D., and Murphy, G. (1994) *J Biol Chem* **269**(21), 14967-14973
36. Boghaert, E. R., Chan, S. K., Zimmer, C., Grobelny, D., Galardy, R. E., Vanaman, T. C., and Zimmer, S. G. (1994) *J Neurooncol* **21**(2), 141-150
37. Galardy, R. E., Grobelny, D., Foellmer, H. G., and Fernandez, L. A. (1994) *Cancer Res* **54**(17), 4715-4718
38. Winding, B., NicAmhlaoibh, R., Misander, H., Hoegh-Andersen, P., Andersen, T. L., Holst-Hansen, C., Heegaard, A. M., Foged, N. T., Brunner, N., and Delaisse, J. M. (2002) *Clin Cancer Res* **8**(6), 1932-1939
39. Solorzano, C. C., Ksontini, R., Pruitt, J. H., Auffenberg, T., Tannahill, C., Galardy, R. E., Schultz, G. P., MacKay, S. L., Copeland, E. M., 3rd, and Moldawer, L. L. (1997) *Shock* **7**(6), 427-431
40. Gijbels, K., Galardy, R. E., and Steinman, L. (1994) *J Clin Invest* **94**(6), 2177-2182
41. Bellahcene, A., Bonjean, K., Fohr, B., Fedarko, N. S., Robey, F. A., Young, M. F., Fisher, L. W., and Castronovo, V. (2000) *Circ Res* **86**(8), 885-891
42. Mandal, M., Mandal, A., Das, S., Chakraborti, T., and Sajal, C. (2003) *Mol Cell Biochem* **252**(1-2), 305-329

FIGURE LEGENDS

Figure 1. BSP binding to MMP-2 does not require the hemopexin domain. Binding interactions between mutant MMP-2 lacking the hemopexin domain and BSP were followed by intrinsic tryptophan fluorescence of the MMP-2 protein (BSP has no tryptophans). 1 nM mutant MMP-2 was reacted with increasing concentration of BSP. Intrinsic tryptophan fluorescence was monitored by excitation at 295 nm and recording emission from 300 to 500 nm using a Photon Technology International Series M fluorimeter (A). Binding saturation was followed by monitoring the change in the area under the emission peak curve (inset). The area under the emission peak curve was used to determine a binding curve by calculating fractional acceptor saturation versus nM BSP added (B) and the corresponding Scatchard plot (C). The binding interaction between BSP and latent MMP-2 (◇), active MMP-2 (O) and mutant hemopexin-free MMP-2 (□) were investigated by solid phase binding assays (D). Scatchard plots derived from solid phase binding assays of BSP and latent MMP-2, active MMP-2 and hemopexin-deleted MMP-2 were determined (E.).

Figure 2. BSP binding to hemopexin-deleted MMP-2 keeps TIMP2 from inhibiting the protease activity. The effect of BSP on the activity of the mutant MMP-2 was profiled using the fluorescein-labeled large molecular weight (gelatin) substrate assay (A). Reaction conditions included mutant MMP2 (□), mutant MMP2 + BSP (O), mutant MMP2 + TIMP2 (△), and mutant MMP2 + TIMP2 +BSP (▲). The effect of a varying substrate concentration on the relative velocity of the mutant enzyme in the presence (O) or absence (□) of BSP was analyzed by linear regression analysis over the first hour and the slope determined at each substrate concentration (B). Similarly, the relative rates of 12.5 μg/ml substrate cleavage by 1.4 nM mutant MMP-2 in the presence of increasing concentrations of TIMP2 were compared by plotting the fluorescent change/min at each dose (C). Conditions included mutant MMP2 alone (□), mutant MMP2 + TIMP2 (△), and mutant MMP2 + TIMP2 + BSP (▲). The effect of BSP on mutant MMP-2 inhibition was studied by titrating a reaction mixture of 10 nM mutant MMP-2 + 10 nM TIMP2 with increasing concentrations of BSP (D). Conditions included mutant MMP2 + TIMP2 (△) and mutant MMP2 + TIMP2 + BSP (▲). The action of BSP on mutant MMP2 activity using a small molecular weight substrate was determined by following pmol product evolution over time (E), velocity plots (F), TIMP2 inhibition curves (G)., and BSP dose response of inhibition by 10 nM TIMP2 + 10 nM mutant MMP-2 (H). Reaction conditions included mutant MMP2 (□), mutant MMP2 + BSP (O), mutant MMP2 + TIMP2 (△), and mutant MMP2 + TIMP2 +BSP (▲). For substrate titrations and TIMP2 dose response, three separate experiments were combined and values plotted present the mean with error bars representing the standard deviation.

Figure 3. BSP effects on TIMP2 inhibition of MMP-2. Small molecular weight substrate was incubated in assay buffer at a final concentration of 100 μM with (A) 10 nM MMP-2 and different concentrations of TIMP2 or (B) 10 nM preformed complex of [MMP-2+BSP] incubated with increasing concentrations of TIMP2, or (C) simultaneously added 10 nM MMP-2 + BSP and different concentrations of TIMP2. TIMP2 concentrations ranged from 0 (□), 1 (O), 5 (△), 10 (◇), and 20 (▽) nM TIMP2. MMP-2 and BSP concentration was 10 nM. Reaction rates were profiled by increasing substrate concentration from 10 to 200 μM. Data from the first six minutes of each reaction condition were used to calculate V_0 (pmols/sec) values. Substrate-velocity plots of MMP-2 incubated with different concentrations of TIMP2 (D), of [MMP-2+BSP] complexes incubated with varying concentrations of TIMP2 (E), or of MMP-2 incubated simultaneously with TIMP2 and BSP (F) were determined. Preformed complexes of [MMP-2+BSP] were formed by incubation at 37°C for 30 minutes prior to addition to the reaction mixture. Six separate experiments were combined for each condition and values shown represent the mean ± the standard deviation.

Figure 4. BSP effects on illomastat (GM6001) inhibition of MMP-2. 100 μM peptide substrate was incubated with 10 nM MMP-2 (□), 10 nM MMP2 + 1 nM illomastat (△), or [10 nM MMP2+10 nM BSP] + 1 nM illomastat (▲) and the evolution of product followed by absorbance at 405 nm (A). In parallel

experiments, peptide substrate was incubated with 10 nM MMP-2 (□), 10 nM MMP2 + 1 nM illomastat (△), or 10 nM MMP2 + 1 nM illomastat + varying concentrations of BSP (▲) to profile a dose response (B). Substrate-velocity plots were generated by increasing substrate concentration at different fixed inhibitor concentrations with the slope over the first six minutes being used to calculate V_0 values (C, D). Active MMP-2 was incubated with illomastat whose concentration varied from 0 (□), 0.1 (○), 0.5 (△), 1 (◇), 5 (▽), and 10 (✣) nM. The inhibitor was added to either directly to MMP-2 (C) or to MMP-2+BSP (D).

Figure 5. BSP stimulates angiogenesis and overcomes MMP-2 inhibitors *in vitro*. HUVEC cells were treated starting on day 6 of culture with vehicle alone (A), 5 nM GM6001 (B), 5 nM TIMP2 (C), 5 nM BSP (D), as well as combinations of 5 nM BSP + 5 nM GM6001 (E) or 5 nM BSP + 5 nM TIMP2 (F). The cells were fixed on day 12 and probed with a PECAM1 antibody (blue) to visualize tubule formation. Note that BSP stimulated tubule formation and in equimolar amounts overcame the inhibitory effects of both natural (TIMP) and synthetic (GM6001) MMP-2 inhibitors.

Figure 6. Quantification of the effects of recombinant BSP on tubule formation and in overcoming the effects of MMP-2 inhibitors. Two distinct fields from each triplicate well of the experimental conditions described were digitized as TIFF files and analyzed using AngioSys Ver. 1.0 software (TCS Cell Works, Buckingham UK). The image analysis package determined the number of tubules (A), the number of branch points or junctions (B) between tubules, as well as the total tubule length in pixels (C). In each case BSP stimulated the angiogenesis parameters even in the presence of the normally inhibitory effect of both natural (TIMP) and synthetic (GM6001) MMP-2 protease inhibitors. In addition a cell surface-associated pool from day 10 cohort cultures was assayed for MMP activity by the large fluorescein-gelatin substrate assay (D) and by zymography (E). Note that BSP caused increased cell surface accumulation of MMP-2 activity in the presence and absence of inhibitors. C, control, B, BSP; T, TIMP2; T+B, TIMP2 + BSP: G, GM6001; G+B, GM6001 + BSP. The region of the zymogram corresponding to active MMP-2 is shown. Asterisks represent ANOVA p values with *, $p \leq 0.05$ and **, $p \leq 0.01$.

TABLES

Table I. BSP & MMP-2 kinetic values.

	K_m	V_{max}	K_{ic}	K_{iu}
mMMP2	96 ± 13	0.20 ± 0.01		
mMMP2+BSP	59 ± 14	0.18 ± 0.02		
MMP2	103 ± 14	1.9 ± 0.1		
MMP2+BSP	90 ± 10	2.1 ± 2		
MMP2+TIMP2	103 ± 9	1.9 ± 0.8	0.67 ± 0.06	1.4 ± 0.2
[MMP2+BSP]+TIMP2	127 ± 18	2.1 ± 0.2	24 ± 12	9 ± 4
MMP2+TIMP2+BSP	98 ± 14	1.8 ± 0.1	10 ± 3	9 ± 2
MMP2+GM6001	106 ± 23	1.8 ± 0.5	0.3 ± 0.1	-
MMP2+BSP+GM6001	88 ± 10	1.6 ± 0.2	9.8 ± 0.3	-

For the small molecular weight substrate peptide substrate, K_m values are μM and for TIMP2 and illomastat the K_I values are nM. Abreviations: mMMP2, mutant hemopexin-deleted MMP-2; BSP, bone sialoprotein; TIMP2, tissue inhibitor of matrix metalloproteinase-2; GM6001, illomastat. K_{ic} and K_{iu} values were determined by fitting the generalized linear mixed inhibition equation and K_I values determined using the equation for competitive inhibition.

FOOTNOTES

[1] The abbreviations used are: SIBLING, Small, Integrin-Binding LIgand, N-linked Glycoprotein; BSP, bone sialoprotein; MMP, matrix metalloproteinase; proMMP, pro-matrix metalloproteinase; TIMP, tissue inhibitor of matrix metalloproteinase; TBS, Tris buffered saline; HRP, horse radish peroxidase; r, binding function; C_S, total ligand concentration; C_A total acceptor concentration; f_a, fractional acceptor saturation.

ACKNOWLEDGEMENTS

This research was supported in part by DAMD 17-02-0684 (N.S.F.) and W81XWH-04-1-0844 (N.S.F.).

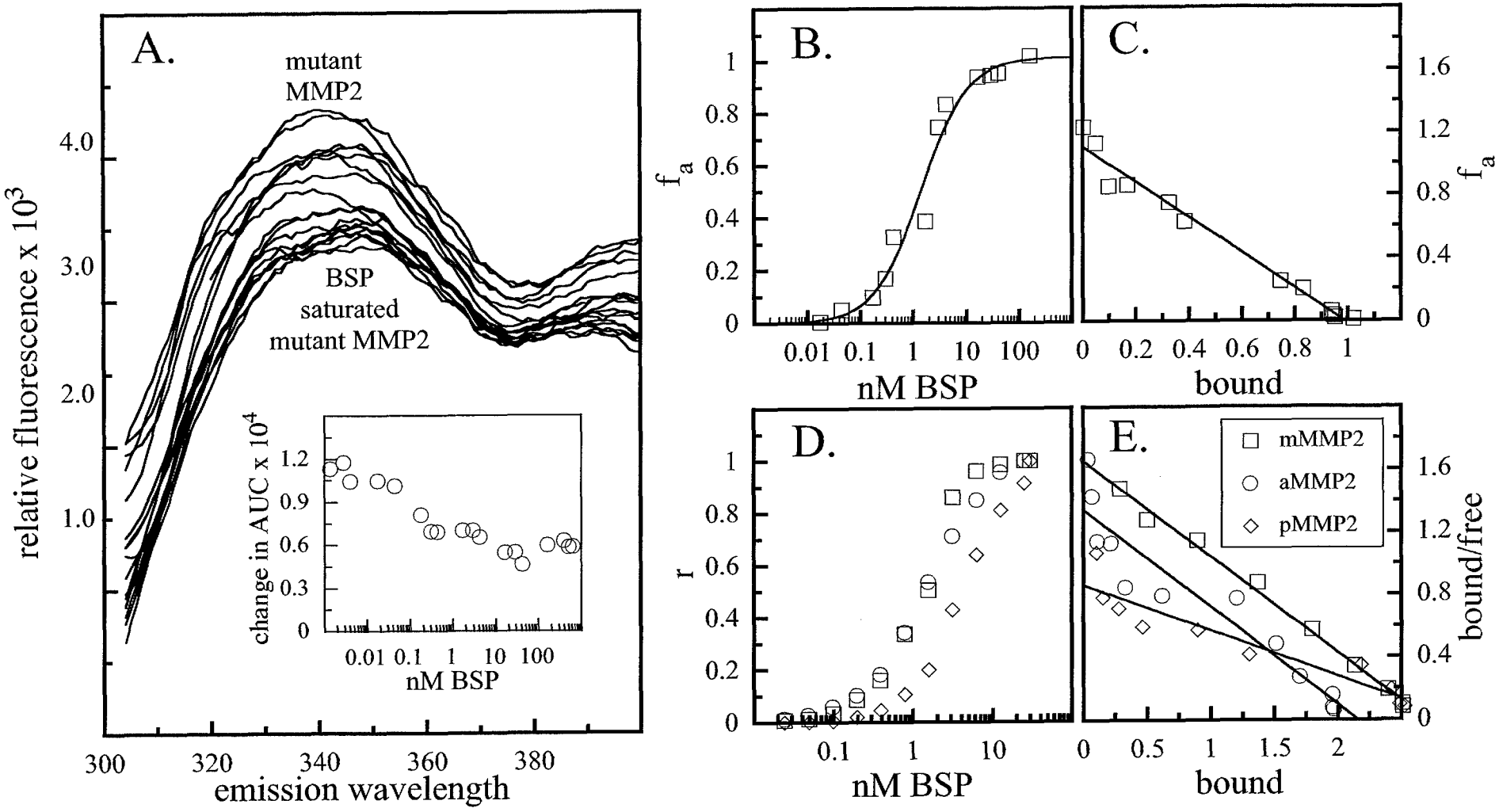
A.
mutant
MMP2
BSP
saturated
mutant MMP2
relative fluorescence x 10^3
emission wavelength
change in AUC x 10^4
nM BSP
B.
f_a
nM BSP
C.
f_a
bound
D.
r
nM BSP
E.
mMMP2
aMMP2
pMMP2
bound/free
bound

Figure 1

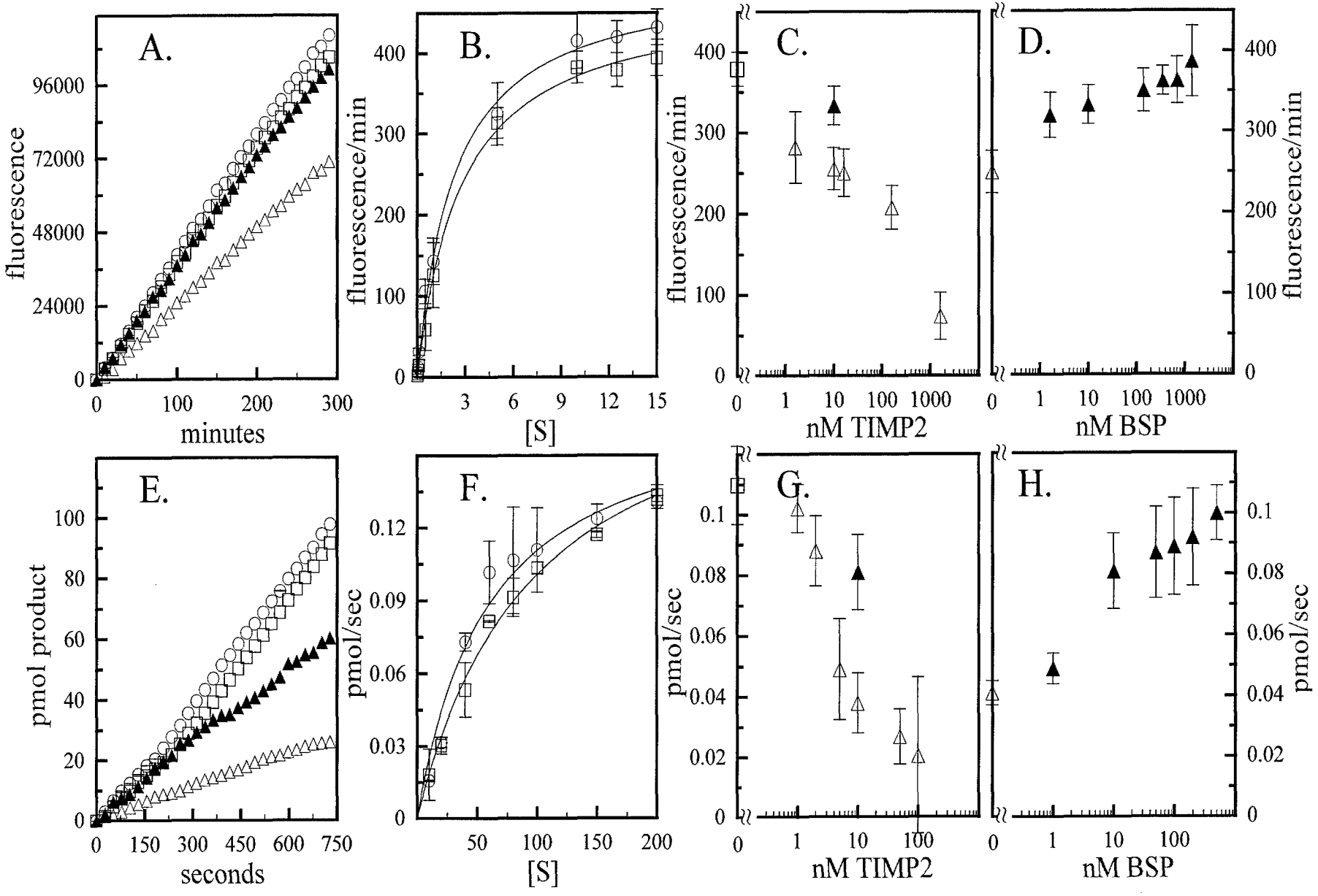
A.
fluorescence
96000
72000
48000
24000
0
0
100
200
300
minutes
B.
fluorescence/min
400
300
200
100
0
3
6
9
12
15
[S]
C.
fluorescence/min
400
300
200
100
0
0
1
10
100
1000
nM TIMP2
D.
400
300
200
100
0
fluorescence/min
0
1
10
100
1000
nM BSP
E.
pmol product
100
80
60
40
20
0
0
150
300
450
600
750
seconds
F.
pmol/sec
0.12
0.09
0.06
0.03
0
50
100
150
200
[S]
G.
pmol/sec
0.1
0.08
0.06
0.04
0.02
0
0
1
10
100
nM TIMP2
H.
0.1
0.08
0.06
0.04
0.02
0
pmol/sec
0
1
10
100
nM BSP

Figure 2

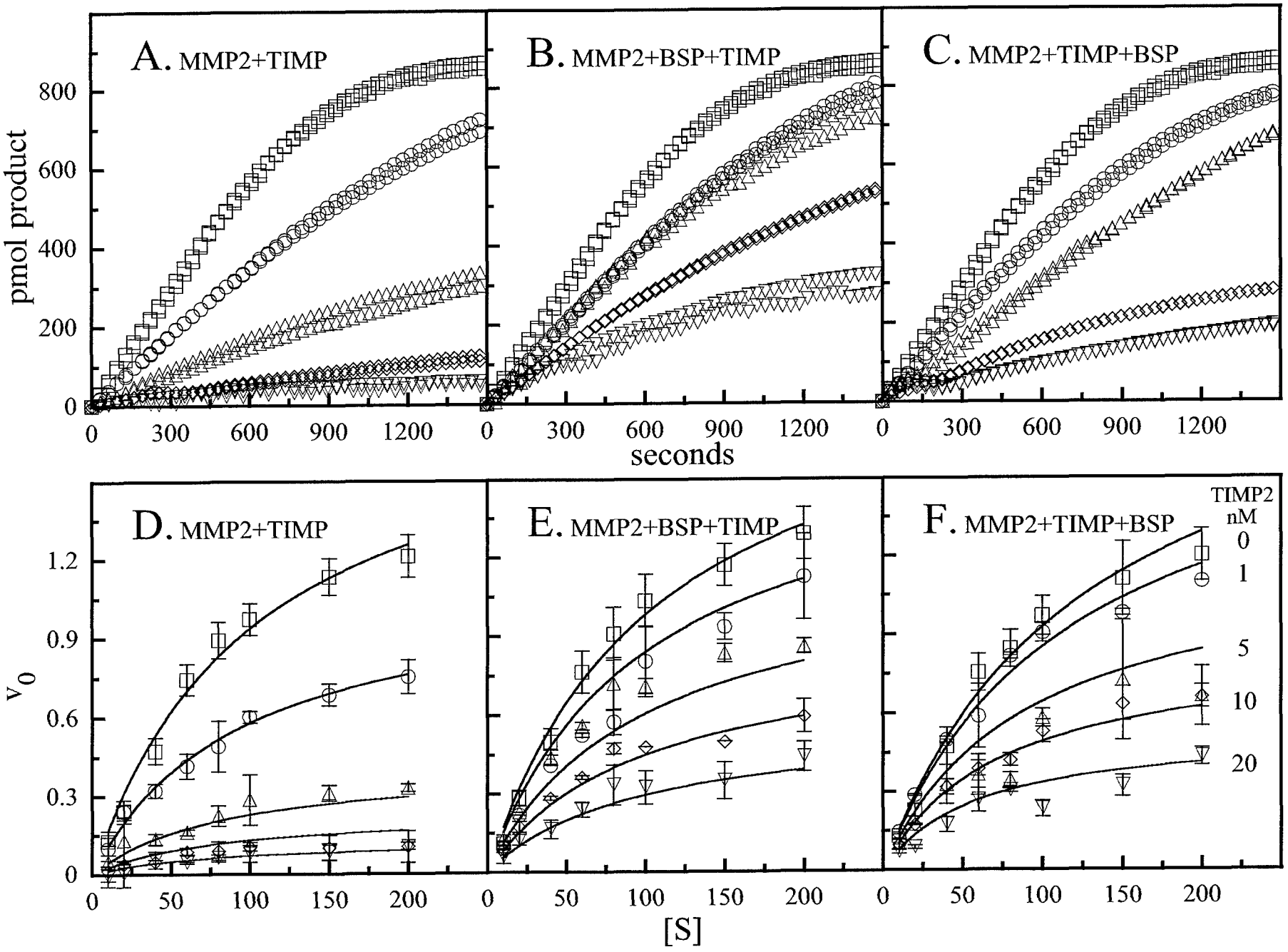
A. MMP2+TIMP
B. MMP2+BSP+TIMP
C. MMP2+TIMP+BSP
pmol product
seconds
D. MMP2+TIMP
E. MMP2+BSP+TIMP
F. MMP2+TIMP+BSP
v_0
[S]
TIMP2 nM
0
1
5
10
20

Figure 3

Figure 4

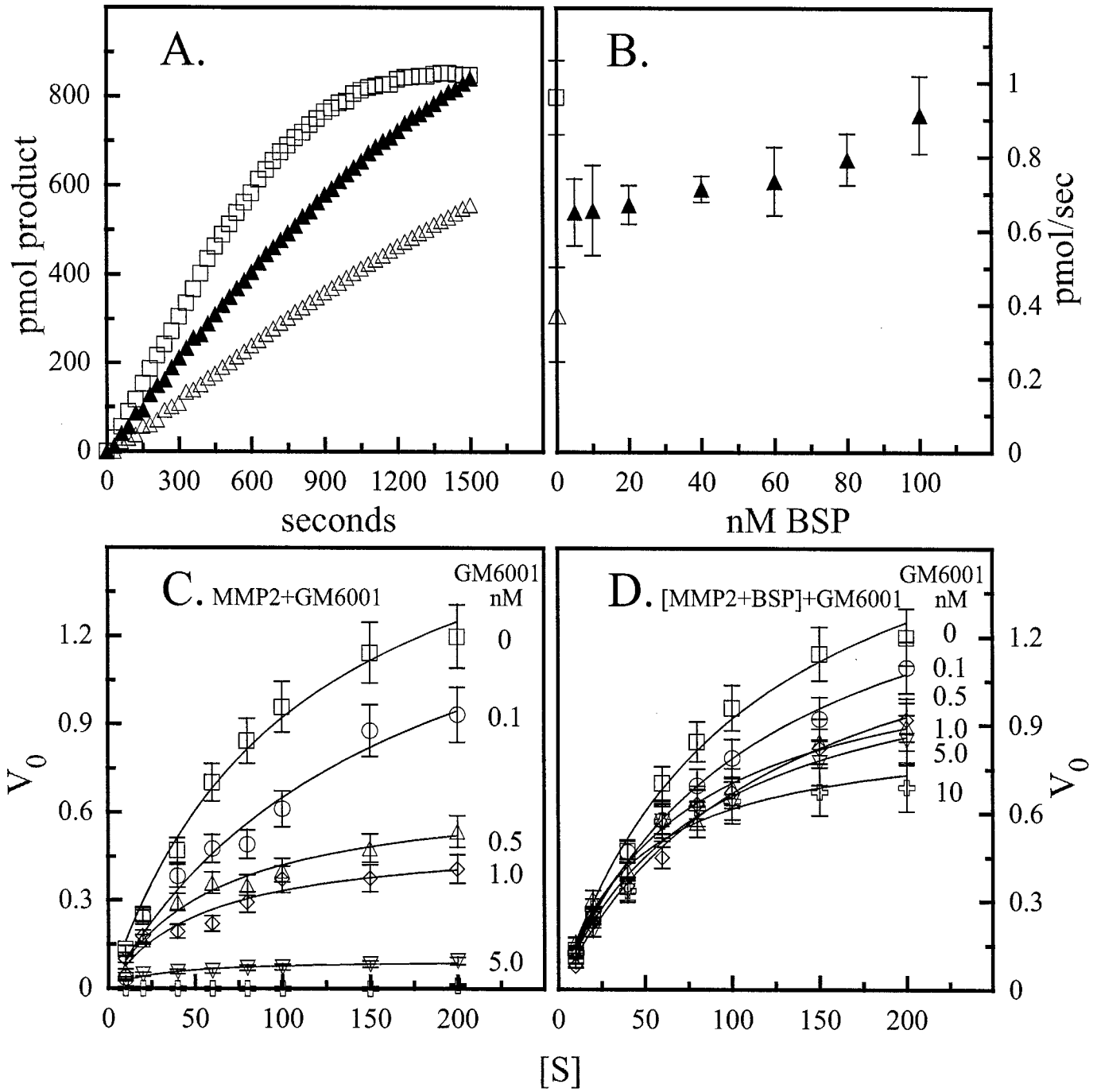
A.
pmol product
seconds
B.
pmol/sec
nM BSP
C. MMP2+GM6001
GM6001 nM
0
0.1
0.5
1.0
5.0
D. [MMP2+BSP]+GM6001
GM6001 nM
0
0.1
0.5
1.0
5.0
10
V0
[S]

Figure 5

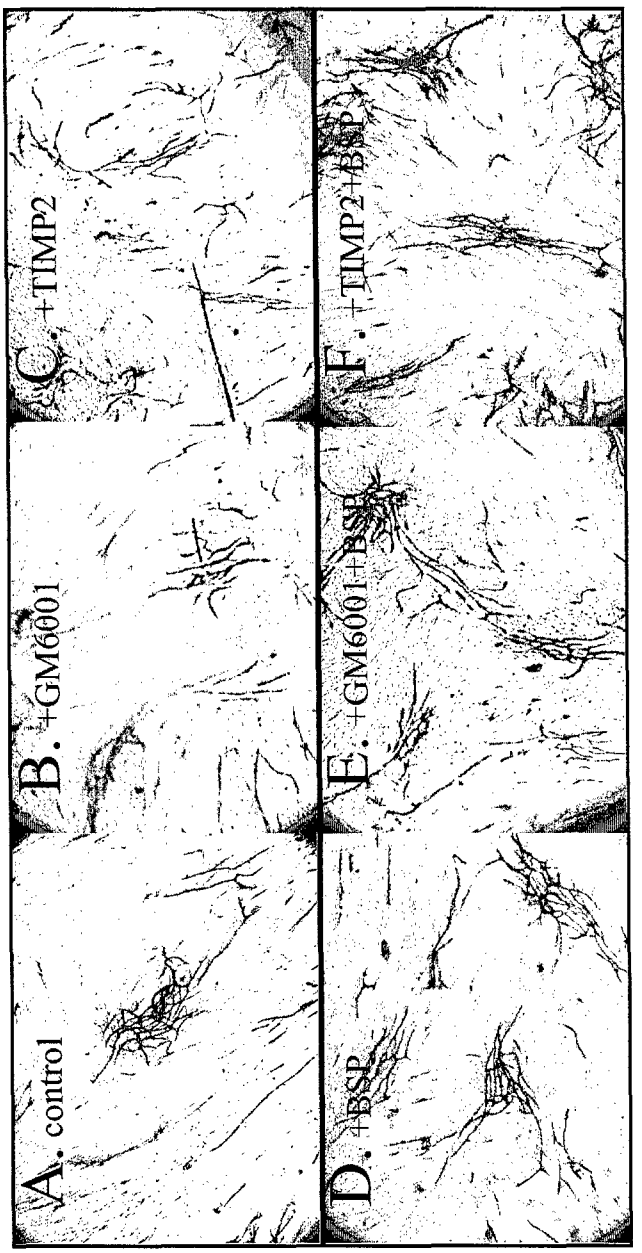

Figure 6

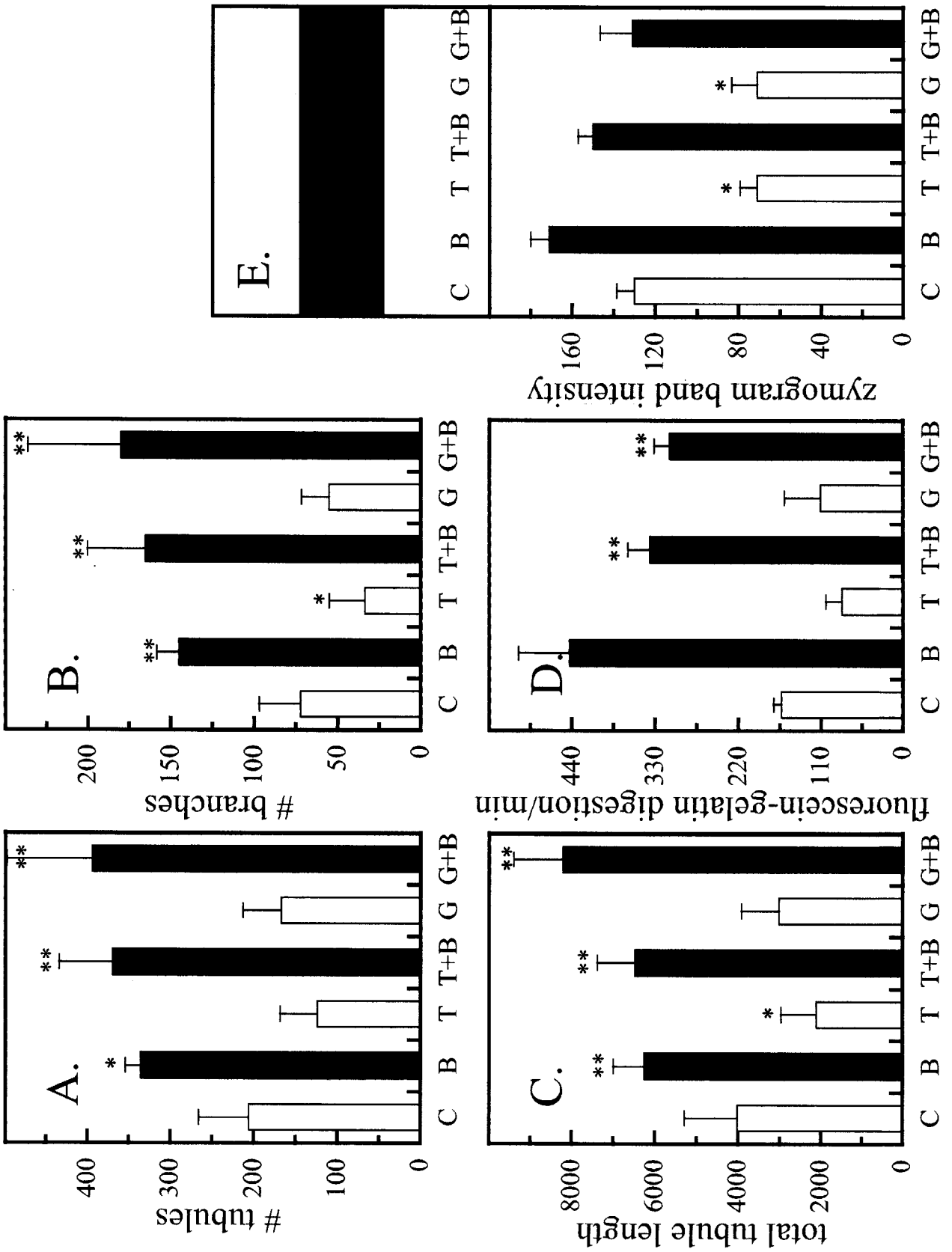
A.
tubules
0
100
200
300
400
C B T T+B G G+B
B.
branches
0
50
100
150
200
C B T T+B G G+B
C.
total tubule length
0
2000
4000
6000
8000
C B T T+B G G+B
D.
fluorescein-gelatin digestion/min
0
110
220
330
440
C B T T+B G G+B
E.
C B T T+B G G+B
zymogram band intensity
0
40
80
120
160
C B T T+B G G+B